Neurogastroenterol Motil (2004) **16,** 335–345 doi: 10.1111/j.1365-2982.2004.00524.x

Diabetic autonomic neuropathy: evidence for apoptosis *in situ* in the rat

C. GUO, A. QUOBATARI, Y. SHANGGUAN, S. HONG, J. W. WILEY & A. QUOBATARI

Department of Internal Medicine, University of Michigan, Ann Arbor, MI, USA

Abstract *We examined the hypothesis that activation of the apoptosis cascade occurs relatively early in diabetes mellitus affecting three distinct neuronal populations that are involved in regulating gut function: (i) dorsal root ganglion (DRG), (ii) vagus nodose ganglion and (iii) colon myenteric plexus.A validated streptozotocin-induced diabetic rat model and age-matched healthy controls were studied. After 4–8 weeks of diabetes the animals were anaesthetized, fixed in situ and the relevant tissues removed. After 1 month of diabetes some animals were treated with insulin for 2 weeks to restore euglycaemia. Apoptosis was measured using immunohistochemical detection of activated caspase-3 and terminal deoxynucleotidyl transferase-mediated dUTP nick-end labelling (TUNEL)-positive cells in adjacent sections in neurones (PGP 9.5-positive cells). The level of apoptosis was confirmed using double-label assessment of caspase-3 and TUNEL in DRG preparations.Caspase-3 immunoreactive neurones demonstrated a range in staining intensity. When all grades of staining were included, 6–8% of the DRG, nodose ganglia and myenteric neurones were immunoreactive in the preparations from diabetic rats compared with 0.2–0.5% in controls. Neurones staining positive for both caspase-3 and TUNEL accounted for 1–2% of the total neuronal population in all three preparations in diabetic rats compared with 0.1–0.2% in controls ($P < 0.05$). Insulin treatment reversed the percentage of TUNEL-positive neurones in diabetic rats to control levels.Activation of the apoptosis cascade occurs relatively early in diabetic autonomic neuropathy and may contribute to the pathophysiology of this disorder.*

Address for correspondence
John W. Wiley, University of Michigan Health System, General Clinical Research Center, A7007 UH, 1500 E Medical Center Dr, Ann Arbor, MI 48109-0108, USA
Tel: (734) 936-8080; fax: (734) 936-4024;
e-mail: jwiley@umich.edu
Received: 31 January 2004
Accepted for publication: 30 March 2004

Keywords *Diabetic neuropathy, apoptosis, autonomic neuropathy, caspases.*

INTRODUCTION

Diabetic neuropathy is the most common peripheral neuropathy in the western hemisphere. Up to 60% of individuals with diabetes mellitus will be afflicted with neuropathy after 20 years from their diagnosis.[1] The pathophysiology of this disorder remains unresolved but is likely multifactorial. Chronic hyperglycaemia associated with diminished insulin production or function appears to be the primary initiating factor in the pathogenesis of diabetic complications. Several hypotheses have been proposed to explain how diabetic complications occur in this milieu including increased activity of aldose reductase, impaired neurotrophin production and function, mitochondrial dysfunction associated with the formation of reactive oxygen species, altered expression/function of protein kinase C (PKC) isoforms, abnormal calcium signalling and formation of advanced glycation end products.[2–8]

Diabetic autonomic neuropathy (DAN) is a well-described complication in long-term diabetes.[1] The DAN is associated with a markedly reduced quality of life and poor prognosis. The manifestations of DAN cause multiple symptoms that can involve the (i) gastrointestinal tract: oesophageal motor dysfunction, diabetic gastroparesis, gall bladder atony, diabetic enteropathy, colonic hypomotility, anorectal dysfunction; (ii) respiratory system: reduced ventilatory drive to hypercapnia/hypoxemia, sleep apnoea; (iii) genitourinary tract: diabetic cystopathy, erectile dysfunction and (iv) cardiovascular system: resting tachycardia, reduced heart rate variability and circadian rhythm of heart rate and blood pressure, painless myocardial ischaemia/infarction, orthostatic hypotension, exercise intolerance, perioperative instability, and sudden death. Previous studies suggest that the function of extrinsic vagal afferent and intrinsic myenteric plexus neural pathways can be impaired

© 2004 Blackwell Publishing Ltd

in animal models of diabetes and patients with long-standing diabetes.[9–11]

Various pathological lesions are observed in animal and human models of diabetes including segmental demyelination, atrophy, loss of myelinated and unmyelinated fibres, Wallerian degeneration, segmental and paranodal demyelination and blunted nerve fibre generation.[12,13] Axonal regeneration in the peripheral nervous system is initially robust, but it eventually fails for unclear reasons. Several animal models have been employed to study the pathophysiology of type 1 and type 11 diabetes mellitus. The most well-established model is the streptozotocin (STZ)-induced diabetic rat model.[2] This model demonstrates many of the complications known to occur in human diabetes.

Recent reports hypothesize that activation of the apoptosis cascade may contribute to the pathophysiology of diabetic peripheral sensory neuropathy. This is an attractive hypothesis because evidence suggests that diabetic sensory neuropathy is associated with mitochondrial dysfunction and formation of reactive oxygen species that are observed with activation of the apoptosis cascade.[4,5,14] In addition, apoptosis has been observed in the hippocampus in the diabetic BB/W rat, a model of type 1 diabetes mellitus.[15] Activation of the apoptosis cascade may also contribute to the pathophysiology of diabetic retinopthy.[16] The 'apoptosis hypothesis' is controversial, however, because the high level of apoptosis reported in some articles employing *in vitro* methods is inconsistent with the slow, progressive natural history of the disease.[4] In addition, counts of the total number of neurones in dorsal root ganglia (DRG) obtained from diabetic and control rats do not support a significant reduction in the total number of soma after long-term diabetes in the STZ-rat model.[17,18] However, if the level of apoptosis *in situ* were relatively low, for example, 1–2% in diabetic peripheral neuropathy, it would be difficult to detect a statistically significant difference in the total number of neurones because the standard error in total cell counts can range from 5 to 10%.[17,18] Most studies evaluating the presence of apoptosis in diabetic neuropathy have examined DRG neurones. We reported previously that 2 weeks of insulin-mediated euglycaemia reversed slowing in nerve conduction velocity, mitochondrial dysfunction and apoptosis observed in DRGs in the STZ-diabetic rat after 1 month of diabetes.[5] The presence of apopotosis has not been evaluated in either vagal afferent (nodose ganglion) or myenteric plexus innervation of the gastrointestinal tract in diabetes mellitus. Both neural pathways play an essential role in regulating gut physiology and have been implicated in the pathophysiology of DAN.[19–26]

Our preliminary studies indicated an *in situ* level of apoptosis of 1–2% in DRG in early (4–8 weeks) diabetic neuropathy using the Terminal deoxynucleotidyl transferase-mediated dUTP nick-end labelling (TUNEL) method to measure apoptosis in the STZ-induced diabetic rat model. The level of apoptosis in controls was significantly less (*c.* 0.1%). The goal of the current study was to confirm and extend our preliminary studies by measuring the *in situ* level of apoptosis in the peripheral nervous system in three distinct neural populations including DRG, nodose ganglion and colon myenteric plexus neurones. Apoptosis was measured in adjacent sections using two techniques, the TUNEL method that detects characteristic nicking of DNA observed in apoptosis and immunoreactive caspase-3 using an antibody that recognizes the activated fragment of the 'executioner' enzyme, caspase-3. Neurones were identified using the neuronal-specific marker PGP 9.5. Some studies were preformed in DRG from control and diabetic rats using double-label immunohistochemistry detection of TUNEL and activated caspase-3 in the same section to confirm the results observed using adjacent slices. Finally, some rats were treated with insulin for 2 weeks after 1 month of diabetes to determine whether apoptosis was reversible in the myenteric plexus similar to what we observed previously in primary afferent (DRG) neurones.

MATERIALS AND METHODS

Reagents

Rabbit polyclonal antibody to cleaved caspase-3 (1 : 50 dilution) was obtained from R&D Biosystems, Minneapolis, MN, USA. The antibody to detect immunoreactive PGP 9.5 was obtained from UltraCone, Isle of Wight, England, UK. The TUNEL-positive cells was assessed according to the manufacturer's instructions using a kit available from Boehringer Mannheim, Mannheim, Germany. Double-label immunohistochemical detection of activated caspase-3 and TUNEL was performed according to the vendors recommended protocol (R&D Systems).

Animal model

All the experiments described in this manuscript were reviewed and approved by the University of Michigan Animal Use Committee. We used male Sprague–Dawley rats, age 4–6 months old for these studies as described previously.[5] Briefly, diabetes mellitus was produced by intraperitoneal injection of STZ

© 2004 Blackwell Publishing Ltd

(45 mg kg^{-1} in citrate buffer, pH 4.5). Age-matched control rats received an intraperitoneal injection of citrate buffer alone. Both groups had free access to rat chow and water. The diabetic rats did not receive insulin and were accepted as diabetic if their fasting glucose levels were >300 mg dL^{-1}. Typically, glucose levels ranged between 350 and 550 mg dL^{-1}. Glucose levels and weights were assessed 3 days after receiving STZ and at the time of euthanasia. Tissue specimens were harvested after 4–8 weeks of diabetes. Our previous studies with this model indicated that rats with diabetes for 4–8 weeks demonstrate a variety of functional abnormalities including delayed nerve conduction velocity, increased calcium influx, impaired inhibitory G-protein function, impaired mitochondrial function and activation of the apoptosis cascade in acutely dissociated DRG neurones.[5,27] Animals were narcotized with carbon dioxide inhalation and immediately perfused with 4% buffered paraformaldehyde for *c.* 20 min via placement of a cardiac catheter. Lower thoracic and lumbar DRGs, nodose ganglia and sections of mid-colon were removed and processed for immunohistochemistry. Some animals were treated with insulin after 1 month of diabetes, using LinBit, a sustained-release insulin implant (2 U day^{-1} implant, Lin Shin, Canada). After the animals were anaesthetized with ketamine and xylazine, the site for implantation was shaved and treated with Betadine solution. Typically, two implants were placed s.c. with a trocar and stylet available from the vendor. Euglycaemia was confirmed by glucose monitoring within 1–2 h after implantation, at *c.* 24 h, and when the animals were killed. Insulin-treated animals were used for experiments after 2 weeks of insulin treatment. Some diabetic animals were treated with sham implants.

Immunohistochemistry

Thoracic and lumbar (T-10, -11 and -12; and L-1 and -2) DRGs and bilateral nodose ganglia were obtained from control and diabetic rats and processed to determine what percentage of PGP 9.5 immunoreactive cells (neurones) were also caspase-3 immunoreactive using an antibody that recognizes the cleaved (activated) 17–19 kDa fragment. The caspase-3 antibody recognizes mouse, rat and human-activated caspase-3. Tissues were embedded in paraffin wax and cut into 4 μm-thick sections. PGP 9.5-positive cells and caspase-3-positive cells were assessed using adjacent sections. A similar approach was used to assess the percentage of PGP 9.5-positive cells that were also TUNEL-positive. Full-thickness sections from the mid-colon were cut in the transverse plane (i.e. perpendicular to the longitudinal muscle layer) and were processed in a similar manner. Sections of mouse breast cancer were processed in parallel and served as a positive control for the caspase-3 and TUNEL assays. Sections not exposed to the primary antibody were processed as negative controls for the assays. Specifically, the fixed tissue specimens were dehydrated with ethanol and xylene and embedded in paraffin by routine methods. Sections from these blocks were then subjected to immunohistochemistry using the anticaspase-3 antibody and labelling with antirabbit IgG conjugated to horseradish peroxidase, followed by development using diaminobenzidine. The primary antibody for PGP 9.5 (1 : 1000 dilution) was conjugated to horseradish peroxidase, followed by development with diaminobenzidine. Assessment of TUNEL-positive and caspase-3-positive cells in preparations from control and diabetic rats was performed in a blinded manner. About 1000 PGP 9.5-positive cells were assessed in each experiment for co-localization with either TUNEL or activated caspase-3 immunoreactivity (IR) in adjacent sections. To avoid duplicate counting of the same cells counting was performed on adjacent sections obtained at 50 μm intervals.

Some studies were performed using DRGs from control and diabetic rats with double-label immunohistochemistry for TUNEL and activated caspase-3 on the same section. The goal of these experiments was to compare the results of the experiments using adjacent sections with an assessment of TUNEL and activated caspase-3 in the same section. These experiments were conducted using a kit from R&D System, Inc., following the manufacturer's protocol. Sections from control and diabetic rats were assessed in a blinded manner. Again, sections were obtained at 50 μm intervals to avoid duplicate counting of the same cells. Assessment of TUNEL and activated caspase-3 immunoreactive cells was confined to soma that demonstrated the typical appearance of DRG neurones.

Evaluation

For activated caspase-3 IR, we used a semiquantitative grading system because cells varied in the intensity of staining. To a first approximation, the grades were as follows: grade 1 – minimal-intensity staining; grade 2 – modest-intensity staining; grade 3 – moderate-intensity staining and grade 4 – high-intensity staining. In the evaluation of TUNEL-positive cells, neurones were considered positive when the nuclei stained positively and showed chromatin clumping. The number of neurones that fulfilled the criteria was expressed as a percentage.

© 2004 Blackwell Publishing Ltd

Analysis

Results were compared as mean ± SE using unpaired, two-tailed Student's *t*-test. Statistical significance was accepted at the $P < 0.05$ level. Statistical analysis was based on the number of animals (n) included in each group.

RESULTS

Animals were studied at 4–6 months of age, 4–8 weeks following induction of diabetes with STZ. The demographic data for the rats employed in the current studies are presented in Table 1. The changes in bodyweight (bw) and blood glucose levels after 4–8 weeks of diabetes were similar to prior studies.[5] Two weeks of insulin treatment after 1 month of diabetes normalized the blood glucose levels and partially reversed the bw differences between control and diabetic rats.

DRG neurones from diabetic rats demonstrated a significant increase in activated caspase-3-positive and TUNEL-positive neurones compared with controls

We routinely performed negative (processed without exposure to the primary antibody) and positive controls for activated caspase-3 immunoreactive cells and TUNEL-positive cells using mouse breast cancer tissue. The positive controls demonstrated reproducible staining in a subpopulation of cells for activated caspase-3 IR and TUNEL that were not observed in the negative controls. Background staining was typically very low or undetectable (data not shown). Fig. 1 depicts the results in DRG from control and diabetic rats. Neuronal soma demonstrated a range of staining intensity for activated caspase-3 that we graded 1 [least intense staining (+)] to 4 [most intense staining (++++)] that are depicted in Fig. 1A, lower left panel (DRG from diabetic rat). Fig. 1A depicts the results in adjacent sections involving PGP 9.5-positive cells (right panels) that were also activated caspase-3-positive (left panels) in DRG from control (top panels) and diabetic (bottom panels) rats. The results are summarized in a histogram presented in Fig. 1B for neurones demonstrating levels 1–4 staining and only level 4 staining for caspase-3-positive neurones. When neurones demonstrating grades 1–4 staining were included in the assessment, caspase-3-positive neurones represented 0.5 ± 0.15% of the total neuronal population in controls and 7 ± 1.8% of the neurones in DRG from diabetic rats ($n = 10$, $P < 0.05$). When assessment of caspase-3-positive neurones was limited to cells that demonstrated only grade 4 staining, 0.15 ± 0.08% of control neurones and 1.6 ± 0.12% of diabetic neurones were caspase-3-positive ($n = 10$, $P < 0.05$). Representative adjacent sections in DRG from control (top panels) and diabetic (bottom panels) rats processed for TUNEL-positive neurones (left panels) and PGP 9.5 (right panels) are depicted in Fig. 1C. Fig. 1D summarizes the TUNEL data in DRG from control and diabetic rats. The TUNEL-positive neurones were detected in 0.10 ± 0.08% of control DRG neurones and 1.8 ± 0.15% of DRG neurones from diabetic rats ($n = 10$, $P < 0.05$).

Activated caspase-3 and TUNEL-positive neurones were significantly increased in nodose ganglia from diabetic rats compared with controls

Fig. 2A depicts the results in adjacent sections involving PGP 9.5-positive cells (right panels) that were also activated caspase-3-positive (left panels) in nodose ganglia from control (top panels) and diabetic (bottom panels) rats. The nodose ganglia obtained from diabetic rats demonstrated variable intensity in capase-3 IR similar to DRG neurones. When neurones demonstra-

Table 1 Bodyweight and blood glucose in insulin-treated or untreated diabetic rats induced by STZ compared with controls

		Body			Blood glucose	
	Sample size (n)	Weight (g)	Age (month)	Duration DM (month)	3 days post-STZ (mg dL^{-1})	Experimental day (mg dL^{-1})
Control	10	354.0 ± 16.9	4.1 ± 0.1	0	88.1 ± 1.9	96.0 ± 1.9
Diabetic	10	338.0 ± 17.5*	4.2 ± 0.1	1.5 ± 0.1	407 ± 22**	464 ± 12**
Diabetic + insulin	4	346.0 ± 15.8	4.2 ± 0.1	1.2 ± 0.1	392 ± 21**	92.0 ± 2.8

Bodyweight, age, duration of diabetic mellitus (DM), and blood glucose 3 days after injection of streptozotocin (STZ) and on the experimental day in non-diabetic control and diabetic STZ rats treated or untreated by insulin. Values are mean ± SD *$P < 0.05$; **$P < 0.01$.

© 2004 Blackwell Publishing Ltd

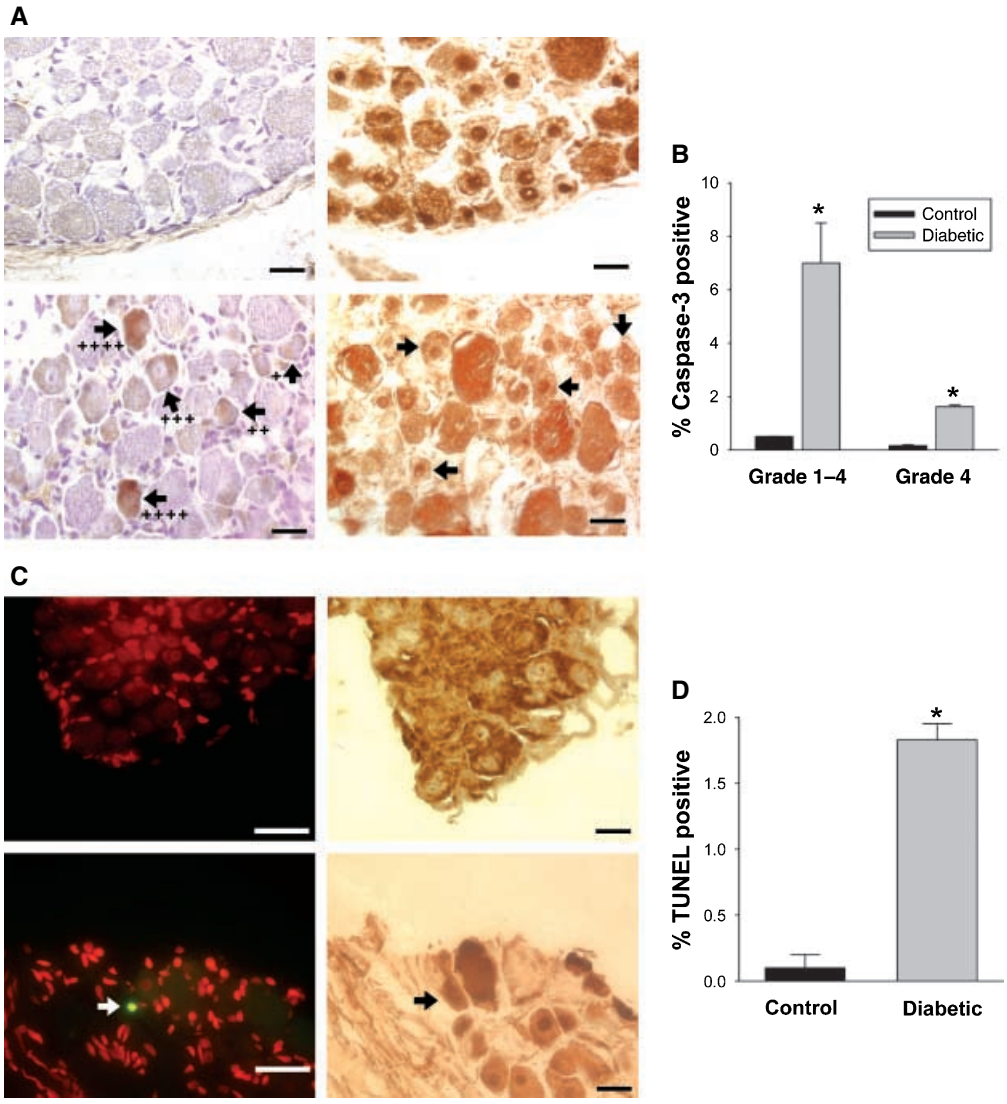

Figure 1 Dorsal root ganglion (DRG) neurones from diabetic rats demonstrated a significant increase in activated caspase-3-positive and terminal deoxynucleotidyl transferase-mediated dUTP nick-end labelling (TUNEL)-positive neurones compared with controls. Neuronal soma demonstrated a range of staining intensity for activated caspase-3 immunoreactivity that we graded 1 [least intense staining (+)] to 4 [most intense staining (++++)] that are depicted in (A), lower left panel (DRG from diabetic rat). (A) Depicts the results in adjacent sections involving PGP 9.5-positive cells (right panels) that were also caspase-3-positive (left panels) in DRG from control (top panels) and diabetic (bottom panels) rats. The results are summarized in a histogram presented in (B) for neurones demonstrating grades 1–4 staining and only grade 4 staining for caspase-3-positive neurones. When neurones demonstrating grades 1–4 staining were included in the assessment, caspase-3-positive neurones represented 0.5 ± 0.15% of the total neuronal population in controls and 7 ± 1.8% of the neurones in DRG from diabetic rats ($n = 10$, $P < 0.05$). When assessment of caspase-3-positive neurones was limited to cells that demonstrated only grade 4 staining, 0.15 ± 0.08% of control neurones and 1.6 ± 0.12% of diabetic neurones were caspase-3-positive ($n = 10$, $P < 0.05$). Representative adjacent sections in DRG from control (top panels) and diabetic (bottom panels) rats processed for TUNEL-positive neurones (left panels) and PGP 9.5 (right panels) are depicted in (C). (D) Summarizes the TUNEL data in DRG from control and diabetic rats. TUNEL-positive neurones were detected in 0.10 ± 0.08% of control neurones and 1.8 ± 0.15% of diabetic neurones ($n = 10$, $P < 0.05$). Scale bar equals 50 μm.

ting grades 1–4 staining were included in the assessment, caspase-3-positive neurones represented 0.4 ± 0.12% of the total neuronal population in controls and 6.2 ± 1.5% of the neurones in DRG from diabetic rats ($n = 10$, $P < 0.05$). When assessment of activated caspase-3 immunoreactive neurones was limited to cells that demonstrated grade 4 staining, 0.18 ± 0.05% of control neurones and 1.4 ± 0.2% of

© 2004 Blackwell Publishing Ltd

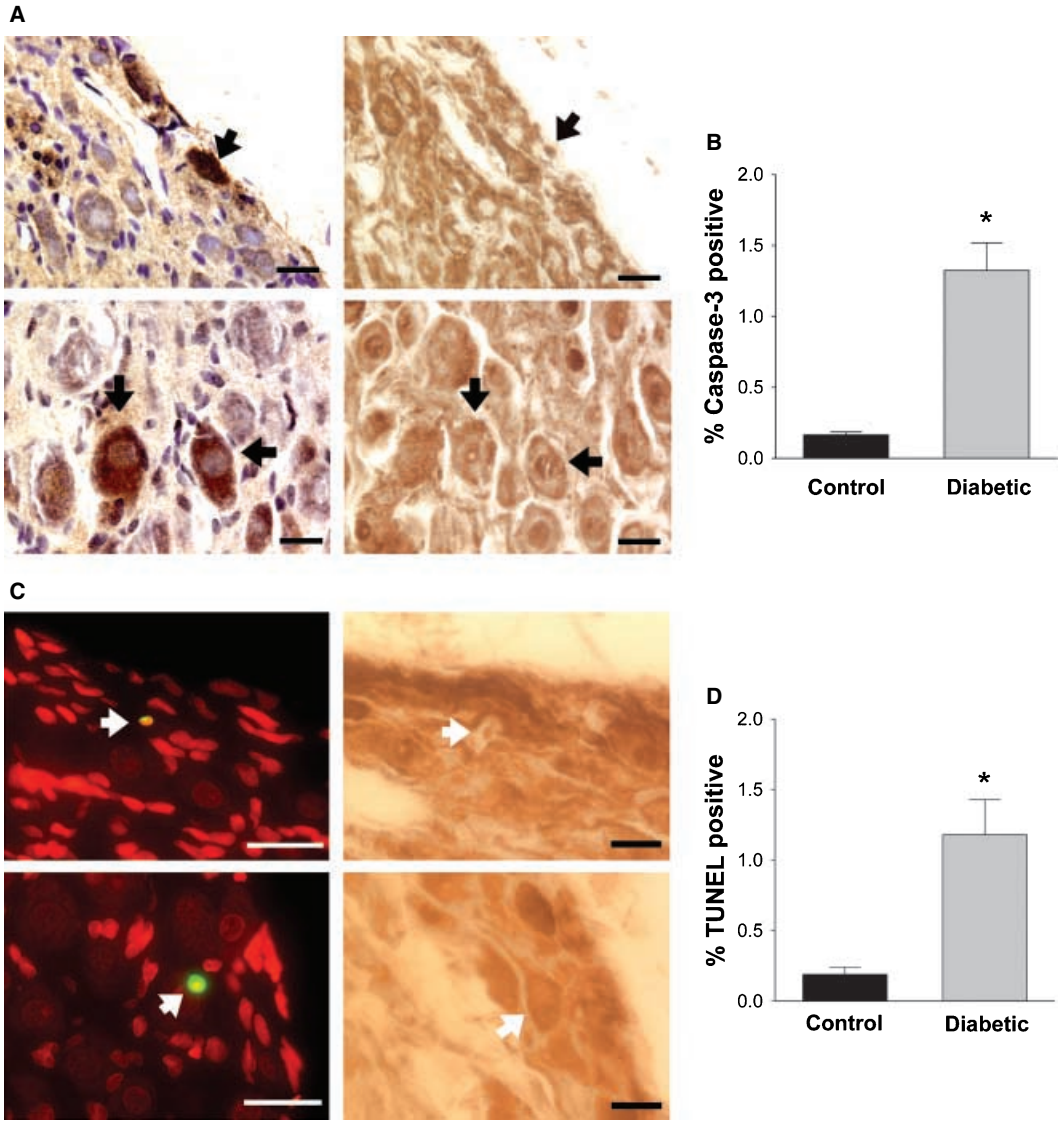

Figure 2 Activated caspase-3 and terminal deoxynucleotidyl transferase-mediated dUTP nick-end labelling (TUNEL)-positive neurones were significantly increased in nodose ganglia from diabetic rats compared with controls. (A) Depicts the results in adjacent sections involving PGP 9.5-positive cells (right panels) that also demonstrated activated caspase-3-positive (left panels) in nodose ganglia from control (top panels) and diabetic (bottom panels) rats. The results are summarized in a histogram presented in (B). When assessment of caspase-3-positive neurones was limited to cells that demonstrated grade 4 staining, 0.18 ± 0.05% of control neurones and 1.4 ± 0.2% of diabetic neurones were caspase-3-positive ($n = 10$, $P < 0.05$). Representative adjacent sections from nodose ganglia from control (top panels) and diabetic (bottom panels) rats processed for TUNEL-positive neurones (left panels) and PGP 9.5 (right panels) are depicted in (C). (D) Summarizes the TUNEL data in nodose ganglia from control and diabetic rats. TUNEL-positive neurones were detected in 0.20 ± 0.08% of control DRG neurones and 1.2 ± 0.2% of DRG neurones from diabetic rats ($n = 10$, $P < 0.05$). Scale bar equals 35 μm.

diabetic neurones were caspase-3-positive ($n = 10$, $P < 0.05$). These results are summarized in a histogram presented in Fig. 2B. Representative adjacent sections from nodose ganglia from control (top panels) and diabetic (bottom panels) rats processed for TUNEL-positive neurones (left panels) and PGP 9.5 (right panels) are depicted in Fig. 2C. Fig. 2D summarizes the TUNEL data in nodose ganglia from control and diabetic rats. TUNEL-positive neurones were detected in 0.20 ± 0.08% of control DRG neurones and 1.2 ± 0.2% of DRG neurones from diabetic rats ($n = 10$, $P < 0.05$).

© 2004 Blackwell Publishing Ltd

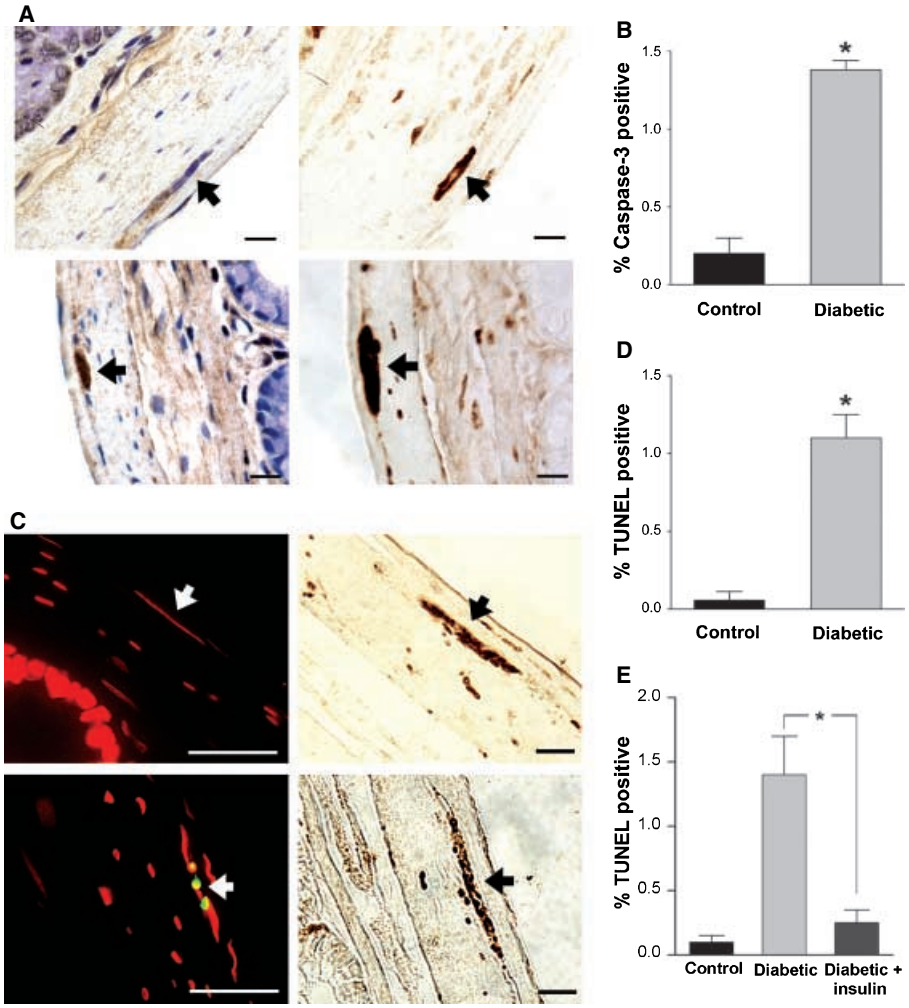

Figure 3 Activated caspase-3 and terminal deoxynucleotidyl transferase-mediated dUTP nick-end labelling (TUNEL)-positive neurones were significantly increased in the colon myenteric plexus from diabetic rats compared with controls and reversed by treatment with insulin. (A) Depicts the results in adjacent sections showing PGP 9.5-positive cells (right panels) that also demonstrated activated caspase-3-positive (left panels) in the colon myenteric plexus from control (top panels) and diabetic (bottom panels) rats. The results are summarized in a histogram presented in (B) for neurones demonstrating grade 4 staining. 0.2 ± 0.1% of control neurones and 1.4 ± 0.08% of diabetic neurones were caspase-3-positive ($n = 10$, $P < 0.05$). Representative adjacent sections of colon from control (top panels) and diabetic (bottom panels) rats processed for TUNEL-positive neurones (left panels) and PGP 9.5 (right panels) are depicted in (C). (D) Summarizes the TUNEL data involving assessment of colon myenteric neurones from control and diabetic rats. TUNEL-positive neurones were detected in 0.08 ± 0.05% of control dorsal root ganglion (DRG) neurones and 1.1 ± 0.15% of DRG neurones from diabetic rats ($n = 10$, $P < 0.05$). (E) After 1 month of diabetes, 2 weeks of insulin-mediated euglycaemia reversed the percentage of TUNEL-positive neurones in the myenteric plexus of diabetic rats to control levels ($n = 4$, $P < 0.05$). Scale bar equals 35 μm.

Activated caspase-3 and TUNEL-positive neurones were significantly increased in the colon myenteric plexus from diabetic rats compared with controls

Fig. 3A depicts the results in adjacent sections showing PGP 9.5-positive cells (right panels) that also demonstrated activated caspase-3-positive (left panels) in the colon myenteric plexus from control (top panels) and diabetic (bottom panels) rats. The results are summarized in a histogram presented in Fig. 3B for neurones demonstrating grade 4 staining, 0.2 ± 0.1% of control neurones and 1.4 ± 0.08% of diabetic neurones were caspase-3-positive ($n = 10$, $P < 0.05$). We found grading the intensity of activated caspase-3 IR in the cross-sections of colon myenteric plexus challenging because many neurones demonstrated a suboptimal surface area of cytoplasm to reliably grade levels 1–3 of

© 2004 Blackwell Publishing Ltd

staining intensity. To a first approximation, the variable intensity of staining observed in DRG and vagus nodose ganglion neurones was also apparent in the colon myenteric neurones. We did observe a level of grade 4 caspase-3 IR neurones (1–2%) and TUNEL-positive neurones in the myenteric plexus that was similar to the nodose ganglion and DRG preparations. Representative adjacent sections of colon from control (top panels) and diabetic (bottom panels) rats processed for TUNEL-positive neurones (left panels) and PGP 9.5 (right panels) are depicted in Fig. 3C. Fig. 3D summarizes the TUNEL data involving assessment of colon myenteric neurones from control and diabetic rats. The TUNEL-positive neurones were detected in 0.08 ± 0.05% of control DRG neurones and 1.1 ± 0.15% of DRG neurones from diabetic rats ($n = 10$, $P < 0.05$). We also examined the effect of 2 weeks of insulin-mediated euglycaemia on the percentage of TUNEL-positive neurones. Insulin treatment was initiated 1 month after onset of diabetes. As depicted in Fig. 4E, insulin treatment reversed the percentage of TUNEL-positive neurones to control levels ($n = 4$, $P < 0.05$).

Double-labelling for activated caspase-3 and TUNEL-positive neurones were increased in DRGs from diabetic rats compared with controls

To confirm the observations generated using adjacent sections we performed double-label immunohistochemistry to detect TUNEL-positive and activated caspase-3-positive neurones in the same section in DRGs from control and diabetic rats. We used DRGs for these confirmatory studies because of the relative ease to identify neuronal soma and quantify the intensity of caspase-3 immunoreactvity to compare with the results using adjacent sections. Sections of mouse breast cancer were processed in parallel and served as a positive control for the double-label assay. Sections not exposed to the primary antibody served as a negative control for the assay. Fig. 4A depicts the positive controls for activated caspase-3 (left panel) and TUNEL, after exposure to TdT enzyme to nick DNA (right panel) using mouse breast cancer tissue. Fig. 4B

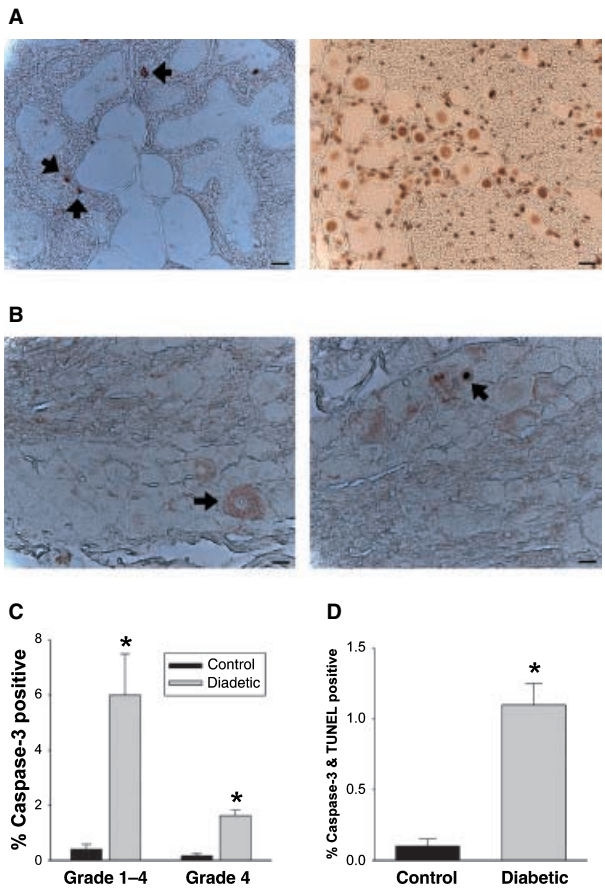

Figure 4 Double-labelling for activated caspase-3 and terminal deoxynucleotidyl transferase-mediated dUTP nick-end labelling (TUNEL)-positive neurones were increased in dorsal root ganglion (DRG) from diabetic rats compared with controls. To confirm the observations generated using adjacent sections, we performed double-label immunohistochemistry to detect TUNEL-positive and activated caspase-3-positive neurones in the same section in DRGs from control and diabetic rats. Sections of mouse breast cancer were processed in parallel and served as a positive control for the double-label assay. Sections not exposed to the primary antibody served as a negative control for the assay. (A) Depicts the positive controls for activated caspase-3 (left panel) and TUNEL, after exposure to TdT enzyme to nick DNA (right panel) using mouse breast cancer tissue. (B) Demonstrates a representative DRG neurone that was activated caspase-3-positive and TUNEL-negative (left panel). Right panel demonstrates a DRG neurone that was both caspase-3-positive and TUNEL-positive. The results of the double-label studies are summarized in histograms presented in (C) for activated caspase-3 immunoreactive neurones. When neurones demonstrating grades 1–4 staining were included in the assessment, caspase-3-positive neurones represented 0.4 ± 0.18% of the total neuronal population in controls and 6 ± 1.5% of the neurones in DRG from diabetic rats. When assessment of caspase-3-positive neurones was limited to cells that demonstrated only grade 4 staining, 0.15 ± 0.08% of control neurones and 1.6 ± 0.2% of diabetic neurones were caspase-3-positive ($n = 10$, $P < 0.05$). (D) Summarizes the double-label data for neurones that were both caspase-3-positive and TUNEL-positive. TUNEL-positive cells typically demonstrated grade 4 and occasionally grade 3-activated caspase-3 immunoreactivity. Neurones that were positive for both caspase-3 and TUNEL were detected in 0.10 ± 08% of control DRG neurones and 1.1 ± 0.15% of DRG neurones from diabetic rats ($n = 10$, $P < 0.05$). Scale bar equals 50 μm.

© 2004 Blackwell Publishing Ltd

(left panel) demonstrates a representative DRG neurone that was activated caspase-3-positive and TUNEL-negative. Fig. 4B (right panel) demonstrates a DRG neurone that was both caspase-3-positive and TUNEL-positive. These results confirm that it is possible to observe activation of caspase-3 without evidence of being TUNEL-positive. The results of the double-label studies are summarized in histograms presented in Fig. C for activated caspase-3-immunoreactive neurones. When neurones demonstrating grades 1–4 staining were included in the assessment, caspase-3-positive neurones represented 0.4 ± 0.18% of the total neuronal population in controls and 6 ± 1.5% of the neurones in DRG from diabetic rats. When assessment of caspase-3-positive neurones was limited to cells that demonstrated only grade 4 staining, 0.15 ± 0.08% of control neurones and 1.6 ± 0.2% of diabetic neurones were caspase-3-positive ($n = 10$, $P < 0.05$). Fig. 4D summarizes the double-label data for neurones that were both caspase-3-positive and TUNEL-positive. The TUNEL-positive cells typically demonstrated grade 4 and occasionally grade 3-activated caspase-3 IR. Neurones that were positive for both caspase-3 and TUNEL were detected in 0.10 ± 08% of control DRG neurones and 1.1 ± 0.15% of DRG neurones from diabetic rats ($n = 10$, $P < 0.05$). Therefore, we observed a significant percentage of neurones that were activated caspase-3-positive but TUNEL-negative in the preparations from diabetic rats. These results were similar to those involving adjacent sections.

DISCUSSION

We believe that this is the first report to assess the level of apoptosis that occurs *in situ* in three peripheral nerve populations in early diabetic neuropathy. Our results extend previous studies in a significant manner by implicating apoptosis as a contributing factor to the complications of diabetes affecting the autonomic nervous system, specifically vagal afferent and myenteric plexus neurones, in addition to DRG neurones. After 1 month of diabetes, 2 weeks of insulin-induced euglycaemia reversed the level of apoptosis observed in the myenteric plexus to control levels. This complements our previous observation in primary afferent (DRG) neurones that insulin treatment can reverse functional abnormalities in early diabetes.

Apoptosis is a regulated cell suicide programme that plays an important role in many biological processes including embryonic development, response to tumours to chemotherapy and the pathogenesis of neurodegenerative diseases.[28] The detection of fragmented DNA strand ends, such as with the TUNEL assay, has been used to characterize apoptotic tissues, but are subject to misinterpretation because necrotic cells also generate fragmented DNA strands.[29] It has also been reported that in some cells DNA fragmentation is reparable and not indicative of certain cell death.[30]

Based on studies of the molecular events in apoptosis, it is generally accepted that cleavage of substrates by caspases is an essential and characteristic feature of activation of the apoptosis cascade.[31] Caspases that participate in the apoptosis cascade have been divided into initiators and executioners. The exact order of the executioners and the position of specific caspases in the apoptotic pathway are still under investigation, but caspases-3, -6, and -7 are generally accepted to be executioners. Caspase-3 is considered a key effector caspase in many cells and mediates the cleavage of itself, other downstream caspases and other caspase substrates. Activation of caspase-3 precedes the fragmentation of DNA detected by TUNEL. It is unclear whether, once activated, the apopotosis cascade is reversible and, if reversible, at what point in the cascade reversibility is lost. We stratified the intensity of activated caspase-3 IR using a 1–4 scale with 1 being the weakest and 4 the most intense staining. Employing this scale, the percentage of neurones with grade 4 caspase-3 IR was similar to the level of apoptosis that we detected using the TUNEL method, i.e. *c.* 1–2%. When we included all levels (grades 1–4) of caspase-3 immunoreactive neurones, the level of caspase-3 activation increased to 6–8%. Our data support that it is possible 'upstream' members of the apoptosis cascade (caspases) can be activated to a greater degree than the terminal events measured by TUNEL. If true, this suggests that it is possible activation of caspase-3 does not commit a cell to obligatory death. For example, in *Caenorhabditis elegans*, CED 3-positive cells (the homologue of mammalian caspase-3) survive and differentiate.[32] It is possible that caspase-independent nuclear fragmentation may occur. For example, hyperglycaemia-mediated nuclear fragmentation was not linked to caspases.[33] Another recent study found that activation of caspase-3 in long-term STZ-induced diabetes may not be inexorably linked to apoptosis.[34] Markers of apoptosis were not increased in DRGs obtained from diabetic rats despite evidence for activation of casapase-3. It is unclear why these results differ from other reports supporting activation of apoptosis in DRGs from diabetic rats although differences in the methods and experimental design may explain these discrepancies. It is relevant that the percentage of activated caspase-3 immunoreactive neurones that we observed with grade 4 staining (1–2%) was similar to that reported in DRGs by

© 2004 Blackwell Publishing Ltd

Schmeichel *et al.*[14] Of interest, the level of apoptosis that this group observed after 1 month and 12 months of diabetes was not significantly different. We reported previously a level of apoptosis of 6–8% in acutely dissociated DRG neurones from early diabetic rats compared with 2–4% in control neurones.[5]. Similar levels of apoptosis were observed by Schmiechel et al.[14] It is possible that the different levels of apoptosis observed in the current study and our previous report are related to the different methods employed to fix the tissue, i.e. *in situ* fixation in the current study *vs* fixation after removal of the tissue in our previous study.

Diabetic neuropathy may be associated with a differential effect on neuronal loss that correlates with the soma size in lumbar DRG neurones.[16] Specifically, morphometric analysis suggested that diabetic neuropathy was associated with preferential drop out (by 43%) of the largest diameter (>50 μm) DRG neurones after 1 year of diabetes. There was no significant difference in total DRG neurone counts. Therefore, the mechanisms influencing neuronal drop out in diabetic neuropathy may preferentially affect peripheral sensory neurones with larger soma.

Diabetic autonomic neuropathy is accompanied by alterations in autonomic and visceral afferent neurones.[1,24] Demyelination of axons in the vagus nerve occurs with diabetic neuropathy. In addition, degeneration and regeneration of unmyelinated vagal nerve fibres have also been reported in patients with diabetic gastropathy. Diabetes affects the content of some but not all neuroactive agents in the nodose ganglion.[26,35] Neurotrophins have been shown to play an important role in the survival and maintenance of peripheral somatic and autonomic neurones.[9,26,36] Therefore, reduced availability and/or function of neurotrophins may contribute to the development and progression of diabetic neuropathy.

A loss of myenteric neurones has been reported in short-term STZ-induced diabetes.[19,20] This effect appears to be more pronounced in the colon compared with the proximal gut.[19,24] The mechanism(s) underlying the loss of neurones were not explored in these reports. These observations along with clinical evidence that colonic motor dysfunction is a relatively early complication in diabetes led us to focus on whether apoptosis is present in the colon myenteric plexus in early diabetic neuropathy.

Assessment of the pathophysiological significance of apoptosis occurring at a level of 1–2% in diabetic neuropathy is a challenging issue. A low level of apoptosis is consistent with the slow, progressive natural history for DAN that typically takes years to become clinically evident. We examined the presence of apoptosis between 4 and 8 weeks after the onset of diabetes, e.g. relatively early in the course of the disease. Additional studies will be required to determine whether the level of apoptosis remains constant over time, increases or decreases. It will also be important to assess whether activation of the apoptosis cascade differentially affects subpopulations of neurones in a region-specific manner.

REFERENCES

1 Ziegler D. Diagnosis and treatment of diabetic autonomic neuropathy. *Curr Diabetes Rep* 2001; **3**: 216–27.
2 Stevens MJ, Dananberg J, Feldman EL *et al.* The linked roles of nitric oxide, aldose reductase, and (Na+, K+)-ATPase in slowing of nerve conduction in the streptozotocin diabetic rat. *J Clin Invest* 1994; **94**: 853–9.
3 Tomlinson DR, Fernyhough P, Diemel LT, Maeda K. Deficient neurotrophic support in the aetiology of diabetic neuropathy. *Diabet Med* 1996; **13**: 679–81.
4 Russell JW, Sullivan KA, Windebank AJ, Herrmann DN, Feldman EL. Neurons undergo apoptosis in animal and cell culture models of diabetes. *Neurobiol Dis* 1999; **6**: 347–63.
5 Srinivasan S, Stevens M, Wiley JW. Diabetic peripheral neuropathy: evidence for apoptosis and associated mitochondrial dysfunction. *Diabetes* 2000; **49**: 1932–8.
6 Hall KE, Sima AAF, Wiley JW. Voltage-dependent calcium currents are enhanced in rat dorsal root ganglion neurons from the Bio/Bred Worchester diabetic rat. *J Physiol* 1995; **486**: 313–22.
7 Ways DK, Sheetz MJ. The role of protein kinase C in the development of the complications of diabetes. *Vitam Horm* 2001; **60**: 149–93.
8 Nishikawa T, Edelstein D, Brownlee M. The missing link: a single unifying mechanism for diabetic complications. *Kidney Int* 2000; **58**: S26–30.
9 Lee PG, Cai F, Helke CJ. Streptozotocin-induced diabetes reduces retrograde axonal transport in the afferent and efferent vagus nerve. *Brain* 2002; **941**: 127–36.
10 Zanoni JN, de Miranda Neto MH, Bazotte RB, de Souza RR. Morphological and quantitative analysis of the neurons of the myenteric plexus of the cecum of streptozotocin-induced diabetic rats. *Arq Neuropsiquiatr* 1997; **55**: 696–702.
11 Buttow NC, Miranda Neto MH, Bazotte RB. Morphological and quantitative study of the myenteric plexus of the duodenum of streptozotocin-induced diabetic rats. *Arq Gastroenterol* 1997; **34**: 34–42.
12 Dyck PJ, Karnes JL, O'Brien P, Okazaki H, Lais A, Engelstad J. The spatial distribution of fiber loss in diabetic polyneuropathy suggests ischemia. *Ann Neurol* 1986; **19**: 440–9.
13 Llewelyn JG, Gilbey SG, Thomas PK, King RH, Muddle JR, Watkins PJ. Sural nerve morphometry in diabetic autonomic and painful sensory neuropathy. A clinicopathological study. *Brain* 1991; **114**: 867–92.
14 Schmeichel A, Schmelzer JD, Low PA. Oxidative injury and apoptosis of dorsal root ganglion neurons in chronic experimental diabetic neuropathy. *Diabetes* 2003; **52**: 165–71.

 © 2004 Blackwell Publishing Ltd

15 Li ZG, Zhang W, Grunberger G, Sima AA. Hippocampal neuronal apoptosis in type 1 diabetes. *Brain Res* 2002; **946**: 221–31.
16 Barber AJ. A new view of diabetic retinopathy: a neurodegenerative disease of the eye. *Prog Neuropsychopharmacol Biol Psychiatry* 2003; **27**: 283–90.
17 Kishi M, Tanabe J, Schmelzer JD, Low PA. Morphometry of dorsal root ganglion in chronic experimental diabetic neuropathy. *Diabetes* 2002; **51**: 819–24.
18 Schmidt RE. Neuronal preservation in the sympathetic ganglia of rats it chronic streptozotocin-induced diabetes. *Brain Res* 2001; **921**: 256–9.
19 Furlan MM, Molinari SL, Miranda Neto MH. Morphoquantitative effects of acute diabetes on the myenteric neurons of the proximal colon of adult rats. *Arq Neuropsiquiatr* 2002; **60**(3-A): 576–81.
20 Fregonesi CE, Miranda-Neto MH, Molinari SL, Zanoni JN. Quantitative study of the myenteric plexus of the stomach of rats with streptozotocin-induced diabetes. *Arq Neuropsiquiatr* 2001; **59**: 50–3.
21 Spangeus A, El-Salhy M. Myenteric plexus of obese diabetic mice an animal model of human type 2 diabetes. *Histol Histopathol* 2001; **16**: 159–65.
22 Hernandes L, Bazotte RB, Gama P, Miranda-Neto MH. Streptozotocin-induced diabetes duration is important to determine changes in the number and basophily of myenteric neurons. *Arq Neuropsiquiatr* 2000; **58**: 1035–9.
23 Spangeus A, Suhr O, El-Salhy M. Diabetic state affects the innervation of gut in an animal model of human type 1 diabetes. *Histol Histopathol* 2000; **15**: 739–44.
24 Furlan MM, de Miranda Neto MH, Sant'ana Dde M, Molinari SL. Number and size of myenteric neurons of the duodenum of adult rats with acute diabetes. *Arq Neuropsiquiatr* 1999; **57**(3B): 740–5.
25 Li Y, Owyang C. Musings on the wanderer: what's new in our understanding of vago-vagal reflexes? V. Remodeling of vagus and enteric neural circuitry after vagal injury. *Am J Physiol Gastrointest Liver Physiol* 2003; **285**: G461–469.
26 Lee PG, Hohman TC, Cai F, Regalia J, Helke CJ. Streptozotocin-induced diabetes causes metabolic changes and alterations in neurotrophin content and retrograde transport in the cervical vagus nerve. *Exp Neurol* 2001; **170**: 149–61.
27 Hall KE, Liu J, Sima AAF, Wiley JW. Impaired inhibitory G protein function contributes to increased calcium levels in rats with diabetic neuropathy. *J Neurophysiol* 2001; **86**: 760–70.
28 Wyllie AH. Apoptosis and the regulation of cell numbers in normal and neoplastic tissues: an overview. *Cancer Metastasis Rev* 1992; **11**: 95–103.
29 Negoescu A, Lorimier P, Labat-Moleur F *et al. In situ* apoptotic cell labeling by the TUNEL method: improvement and evaluation of cell preparations. *J Histochem Cytochem* 1996; **44**: 959–68.
30 deBoer RA, van Veldhuisen DJ, van der Wijk J *et al.* Additional use of immunostaining for active caspase 3 and cleaved actin and PARP fragments to detect apoptosis in patients with chronic heart failure. *J Card Fail* 2000; **6**: 330–7.
31 Green DR. Apoptotic pathways: paper wraps stone blunts scissor. *Cell* 2000; **102**: 1–4.
32 Reddien PW, Caneron S, Horvitz HR. Phagocytosis promotes programmed cell death in *C. elegans*. *Nature* 2001; **412**: 198–202.
33 Hick L, Van Der Smissen P, Heusterpreute M, Donnay I, De Hertogh R, Pampfer S. Identification of caspase-3 and caspase-activated deoxyribonuclease in rat blastocysts and their implication in the induction of chromatin degradation (but not nuclear fragmentation by high glucose. *Bio Reprod* 2001; **64**: 555–62.
34 Cheng C, Zochodne DW. Sensory neurons with activated caspase-3 survive long-term experimental diabetes. *Diabetes* 2003; **52**: 2363–71.
35 Yu O, Ouyang A. Substance P binding in gastrointestinal tract of nondiabetic BB rat and changes in diabetic BB rat over time. *Dig Dis Sci* 1999; **44**: 749–55.
36 Unger JW, Klitzsch T, Pera S, Reiter R. Nerve growth factor (NGF) and diabetic neuropathy in the rat: morphological investigations of sural nerve, dorsal root ganglion and spinal cord. *Exp Neurol* 1998; **153**: 23–34.

© 2004 Blackwell Publishing Ltd